Clays and Clay Minerals, Vol. 46, No. 5, 509–520, 1998.

VERMICULAR KAOLINITE EPITACTIC ON PRIMARY PHYLLOSILICATES IN THE WEATHERING PROFILES OF ANORTHOSITE

GI YOUNG JEONG

Department of Earth and Environmental Sciences, Andong National University, Andong 760-749, Korea

Abstract—The microtextural changes in the kaolinization of primary phyllosilicates including biotite, sericite, clinochlore and muscovite were investigated by scanning electron microscopy (SEM) and microchemical analysis of thin sections of weathered anorthosite. Kaolinization began at grain edges and propagated toward the interior. Grains were highly fanned out from the edges and exfoliated into several flakes along the basal cleavages, producing lenticular voids. Finally, long vermicular kaolinite pseudomorphs were formed after primary phyllosilicates. Statistical analysis showed a ninefold increase in volume during the kaolinization of biotite, suggesting that most Al in the kaolinite was imported from ambient weathering solution. Weathering primary phyllosilicates supplied templates suitable for the thick epitactic overgrowth of kaolinite to form long vermicular pseudomorphs. Al was sufficiently available due to the intense weathering of soluble anorthosite. Although present in small amounts, primary phyllosilicates gave high volumetric and mineralogical contributions to the weathering profiles by facilitating kaolinite precipitation.

Key Words—Epitactic, Kaolinite, Pseudomorph, Scanning Electron Microscopy, Weathering.

INTRODUCTION

Phyllosilicates are common constituents of bedrock and overlying soils. With progressive weathering, primary phyllosilicates alter into secondary minerals, displaying a sequential change of textures, chemistry and mineralogy. Diverse alteration sequences have been reported, depending on the local weathering environment. Under well-drained weathering conditions, primary phyllosilicates ultimately alter into kaolinite with or without intermediate phases such as vermiculite, smectite or mixed-layered clay minerals (Coffman and Fanning 1975; Stoch and Sikora 1976; Eswaran and Bin 1978; Gilkes and Suddhiprakarn 1979a, 1979b; Harris, Zelazny and Bloss 1985; Harris, Zelazny, Baker and Montens 1985; Rebertus et al. 1986; Ahn and Peacor 1987; Banfield and Eggleton 1988, 1990; Singh and Gilkes 1991; Cho and Mermut 1992). High-resolution transmission electron microscopic (TEM) studies have well elucidated the detailed kaolinization process of primary phyllosilicates such as topotactic (Ahn and Peacor 1987; Jiang and Peacor 1991; Singh and Gilkes 1991; Robertson and Eggleton 1991) and epitactic replacement (Banfield and Eggleton 1988, 1990; Singh and Gilkes 1991). One of the distinct features of the alteration is the formation of pseudomorphs after primary phyllosilicates. It is generally reported that volume is preserved or reduced during the kaolinization of biotite, supporting Al-conservation (Stoch and Sikora 1976; Harris, Zelazny and Bloss 1985; Rebertus et al. 1986; Banfield and Eggleton 1988). However, the literature also describes the fanning-out of flakes along the basal cleavages (Gilkes and Suddhiprakarn 1979a; Fordham 1990; Nahon 1991), but little attention has been given to the kaolinite pseudomorphs, which are increased in size compared to the original grain. Large kaolinite pseudomorphs derived from small primary phyllosilicates might have implications for the behavior of elements and the formation process of kaolinite in the weathering profiles. During a study of the kaolin formed by the deep residual weathering of anorthosite in the Sancheong kaolin deposits, Korea, it was found that biotite, sericite, clinochlore and muscovite were altered into vermicular kaolinite, typically displaying fanning-out textures involving an enormous increase in volume. The microtextural and mineralogical changes throughout the kaolinization of primary phyllosilicates were investigated by SEM and microchemical analysis of petrographic thin sections prepared from undisturbed weathering products. This paper reports the formation process of vermicular kaolinite pseudomorphs after primary phyllosilicates in the anorthosite and their implications for the kaolinic weathering profiles.

ANORTHOSITE AND RELATED KAOLIN DEPOSITS

Anorthosite intruded a Precambrian gneiss complex in the Sancheong district, Korea, and cropped out as a square mass (12 × 14 km). The Sm-Nd isotopic age of anorthosite intrusion was 1678 ± 90 Ma (Kwon and Jeong 1990). Microfractures were well developed in anorthosite as a result of the cataclastic deformation during the regional metamorphism after intrusion. Anorthosite is composed almost wholly of medium- to coarse-grained labradorite plagioclase (normally above 95 vol%) with minor hornblende, epidote, zoisite, ilmenite, titanite and primary phyllosilicates including biotite, sericite, clinochlore and muscovite (Jeong 1992). Relative contents of primary phyllosilicates in

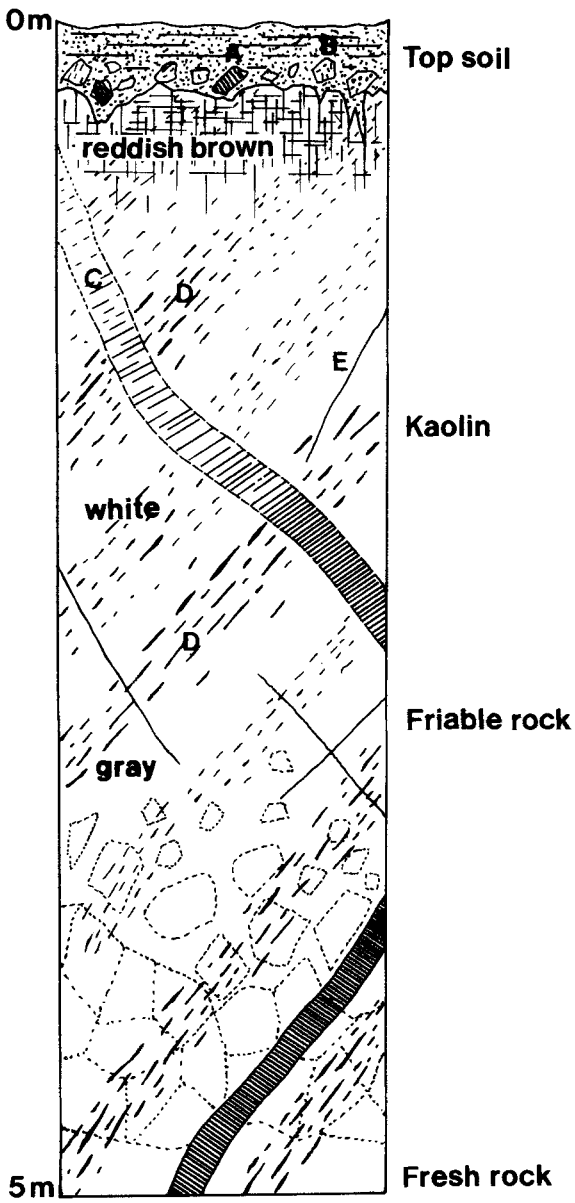

Figure 1. A schematic sketch of the anorthosite weathering profile. Fresh rock changes into white and reddish brown kaolin through friable rock, preserving the original rock structures. Uppermost soils are disturbed by lateral transportation. Key: A = block of weathered dike rock; B = block of weathered kaolin; C = weathered dike rock; D = laminations or spots of the aggregates of mafic minerals; E = halloysite veinlets.

the study area were difficult to estimate due to their small absolute contents but extensive thin section examination showed that biotite was most common (about 1 vol%) whereas sericite, clinochlore and muscovite were relatively rare in decreasing order. Primary phyllosilicates occurred as thin fillings in the microfractures or as randomly oriented aggregates in the mafic spots of anorthosite together with hornblende, zoisite and titanite. Structural formulas of primary phyllosilicates determined from electron probe micro analysis (EPMA) data (Tables 2, 4 and 5) are $K_{1.70}Na_{0.05}Ca_{0.02}(Fe^{II}_{2.13}Mg_{3.08}Ti_{0.08}Al_{0.57}Cr_{0.02})_{5.88}(Si_{5.70}Al_{2.30})_8O_{20}(OH)_4$ (biotite), $(Al_{2.57}Fe^{II}_{4.25}Mg_{5.11}Mn_{0.04})_{11.97}(Si_{5.46}Al_{2.54})_8O_{20}(OH)_{16}$ (clinochlore), $K_{1.94}Na_{0.09}(Fe^{II}_{0.29}Mg_{0.25}Ti_{0.03}Al_{3.42})_4(Si_{6.20}Al_{1.80})_8O_{20}(OH)_4$ (muscovite), respectively.

The kaolin deposits were formed by the residual saprolitic weathering of the anorthosite under humid temperate climate with mean annual precipitation of 1354 mm and mean air temperature of 12.7 °C (Korea Meteorological Service 1985). Most kaolin deposits were developed on the mountainsides of low slope (less than 22°). Good drainage of the slope indicated their formation under oxidizing environment. The age of the kaolin deposits could not be accurately dated, but their occurrences suggested relatively young weathering products. The kaolin deposits have been an important source of kaolin used for ceramic raw materials in Korea. The kaolins consist mostly of kaolinite and halloysite in various proportions (Jeong 1992). Kaolinites have been formed by direct precipitation from solution in microfractures of plagioclase or replacement for primary phyllosilicates, which are the object of this study. A schematic sketch of the anorthosite weathering profiles studied is given in Figure 1. The fresh rock gradually changed into kaolin through thick, partially weathered, friable rocks. Highly weathered anorthosite containing plagioclase below 20 wt% is provisionally termed "kaolin" in this study. Good preservation of the original rock fabrics without severe disturbance was one of the remarkable characteristics of the anorthosite weathering profiles, implying little volume change during weathering. Laminations of mafic minerals, dikes, joints and quartz veins in anorthosite mass were extended throughout the weathering profiles without any notable change of their orientations and widths (Figure 1).

MATERIALS AND EXPERIMENTAL METHODS

Partially weathered anorthosites and mature kaolin samples were collected from the weathering profile exposed at the kaolin mine in the Sancheong district. Samples were stored in polyethylene bottles to preserve the original textures. Mineral compositions of bulk samples and weathering products of primary phyllosilicates were determined with a Rigaku RAD3-C X-ray diffractometer equipped with Cu tube operating at 35 kV/20 mA. Weathered biotite and clinochlore grains were separated by magnetic separator and handpicking under stereomicroscope and thoroughly washed in distilled water with ultrasonic agitation. The whole range of mineralogical changes was most finely observed in the grains presently undergoing active alteration rather than in the almost completely altered

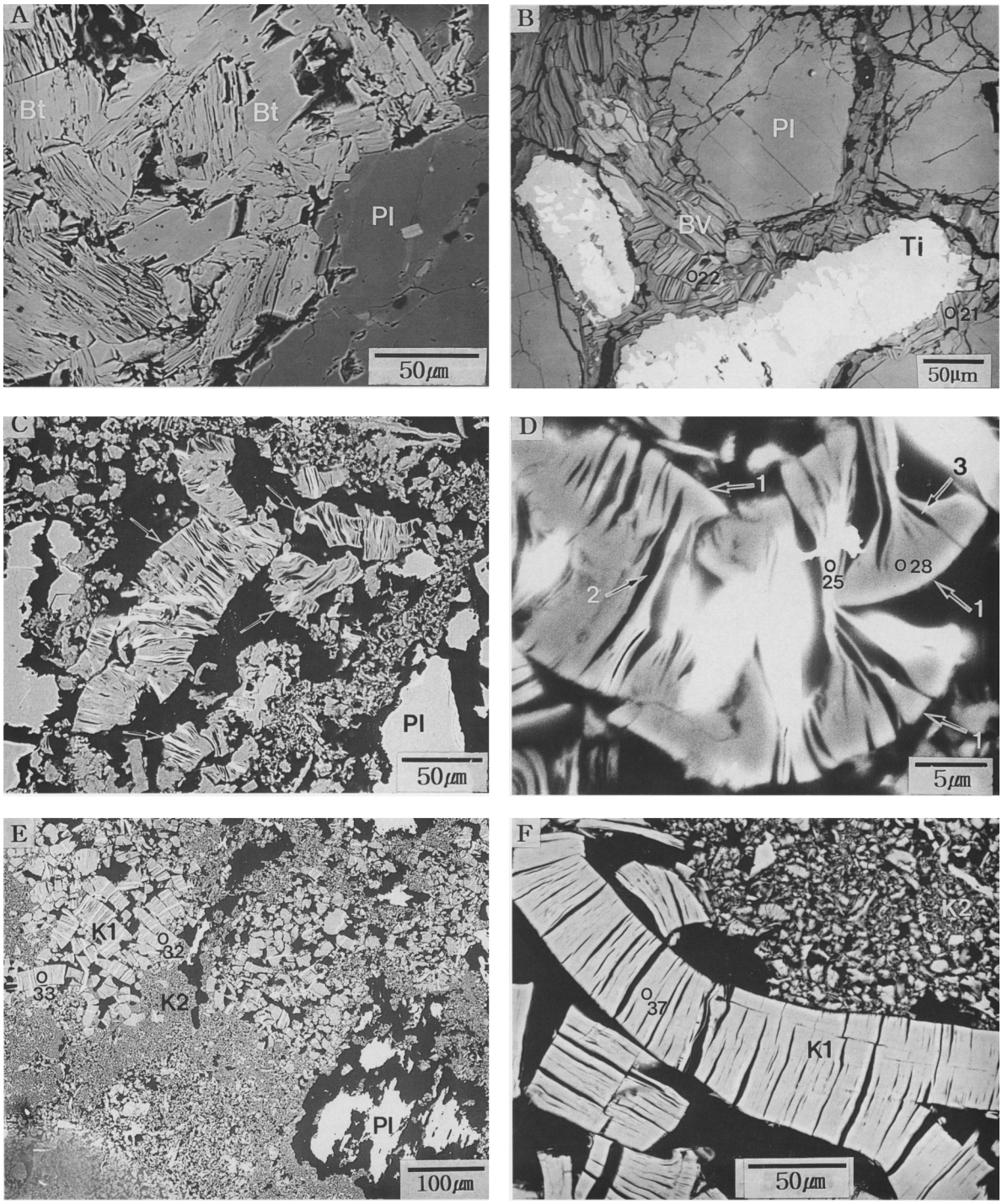

Figure 2. Scanning electron micrographs of thin sections showing the kaolinization process of biotite. A) Biotite (Bt) in fresh anorthosite showing the interlocking grain fabric. Pl = plagioclase. B) Biotite altering to a biotite–vermiculite mixed-layer mineral and vermiculite (BV) in the very slightly weathered friable rock. Ti = titanite. C) Kaolinizing biotite grains (arrows) in moderately weathered friable rock (plagioclase 46%). D) Magnified view of kaolinizing biotite grains showing the great fanning-out (arrow 1) from edges and exfoliation. Note the large lenticular voids separating flakes (arrow 2) and small voids in the fan (arrow 3). E) Aggregates of vermicular kaolinite pseudomorphs (K1) after biotite surrounded with small kaolinite grains (K2) in kaolin (plagioclase 11%). Note the skeletal plagioclase (Pl). F) Large vermicular kaolinite pseudomorph (K1) after biotite. Note the relatively small size of vermicular kaolinite (K2) directly formed from weathering solution. Black = voids. Numbers beside open circle in B), D), E) and F) indicate the points analyzed by EPMA in Table 2.

https://doi.org/10.1346/CCMN.1998.0460504 Published online by Cambridge University Press

Table 1. Bulk chemistry and mineral composition of samples (unit in wt%).

Sample	No.	SiO_2	Al_2O_3	Fe_2O_3	MgO	TiO_2	MnO	K_2O	Na_2O	CaO	Total	Depth (m)	Pl	K	H	V	S
Kaolin	J894	46.62	36.49	1.53	0.26	0.15	0.02	0.45	0.50	1.20	87.22	0.3	11	53	27	0	6
Friable rock	J892	48.24	32.05	2.09	0.69	0.17	0.03	0.39	2.01	5.36	91.03	1.8	46	35	3	6	5
Friable rock	J891	51.70	29.70	0.92	0.24	0.20	0.03	0.30	4.15	12.06	99.30	4.2	95	nd	nd	nd	nd
Fresh rock	J890	52.58	28.72	0.76	0.25	0.19	0.02	0.32	4.31	12.04	99.19	5.5	95	nd	nd	nd	nd

Key: Pl = plagioclase; K = kaolinite; H = halloysite; V = vermiculite; S = smectite; nd = not determined.

grains. Sericite was separated from <0.5 μm size fraction of kaolin by the selective dissolution of kaolinite and halloysite using hot 5 *N* NaOH solution (Konta 1972). For a textural study of the weathering primary phyllosilicates, air-dried samples were impregnated with Araldite epoxy resin under vaccum. Polished thin sections were prepared and coated with carbon. The microtextures of thin sections were observed using a Hitachi S2500 scanning electron microscope in a secondary electron image mode. To optimize the contrast of the image of flat surface, a large condenser lens aperture was inserted and condenser lens current was reduced as low as possible. Qualitative chemical analysis of minerals was carried out with a Kevex energy dispersive X-ray spectrometer (EDS) during the observation. Quantitative chemical analysis was carried out with a JEOL 733 electron probe microanalyzer (EPMA) at 15 kV using an electron beam of 5 mA (current) and 1 μm (diameter). Whole-rock chemistry of the sample was determined with a Philips PW1480 X-ray fluorescence (XRF) spectrometer at the Korea Basic Science Institute. Relative contents of minerals of the samples were determined by the combination of X-ray diffraction (XRD) peak intensities, whole-rock chemistry and mineral chemistry. For example, the plagioclase content could be obtained from the EPMA data of plagioclase and the XRF data of the sample because the Na_2O content of whole-rock chemistry was assigned to plagioclase. Plagioclase content of the samples represents the weathering degree of anorthosite. Samples studied are described in Table 1.

RESULTS

Biotite Kaolinization

In fresh rock, the biotite had a dark brown color and shiny appearance. Biotite grains were complexly interlocked with each other, forming an aggregate in the grain boundary or microfracture (Figure 2A). Biotite consisted of several flakes separated by basal cleav-

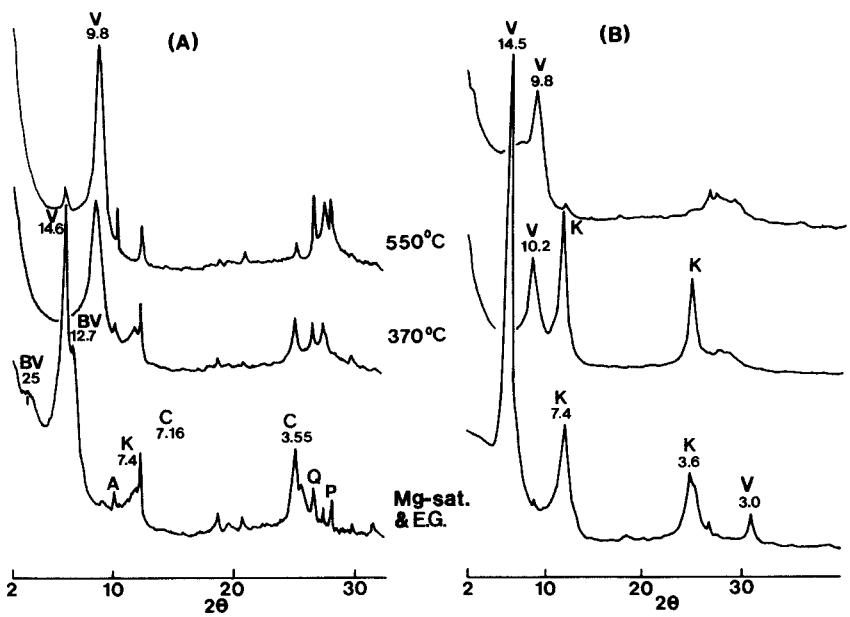

Figure 3. X-ray diffraction patterns of kaolinizing biotite in very slightly weathered friable rock (A) and in moderately weathered friable rock (plagioclase 46%) (B). Oriented mounts. Key: BV = biotite–vermiculite mixed layer; V = vermiculite; K = kaolinite; C = chlorite; Q = quartz; P = plagioclase, A = amphibole.

https://doi.org/10.1346/CCMN.1998.0460504 Published online by Cambridge University Press

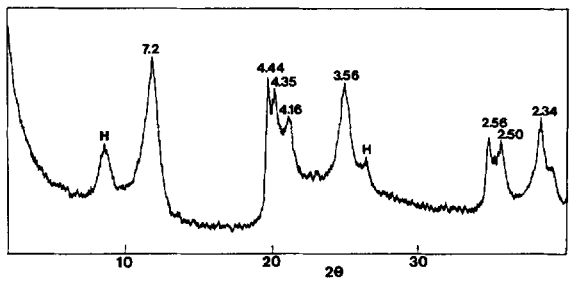

Figure 4. XRD pattern of kaolinized biotite in kaolin. Random mounts. Key: H = halloysite.

ages. Each flake was straight, without fanning at the edges. In very slightly weathered friable rock (plagioclase 95%) where plagioclase remains intact, biotite grains were altered to a yellowish brown color. Weathered biotite grains were still interlocked (Figure 2B) but consisted mostly of biotite–vermiculite mixed-layer mineral (B–V) and vermiculite with minor amounts of kaolinite (Figure 3A). The K_2O content of the weathered grains decreased to 1–2 wt%, whereas Fe_2O_3 and MgO contents were still high, implying a microscale mixture of B–V and vermiculite (analysis No. 21, 22 in Table 2). In moderately weathered friable rock (plagioclase 46%), weathered biotite grains were highly expanded along the *c*-axis (Figure 2C) and consisted mostly of vermiculite and kaolinite with minor amounts of B–V (Figure 3B). The *d*–values of *(001)* peak of kaolinite at 7.4 Å indicated a small layer number along the *c*-axis (about 6 to 7 layers) (Brindley 1980). The weathered biotite grains were separated into several flakes by long lenticular voids (Figure 2D). Each flake was again cleaved into more thin flakes and fanned out toward the edges, producing small lenticular voids. EPMA analyses showed that fanned edges were essentially kaolinite (analysis No. 26, 27, 28 in Table 2), whereas unfanned interiors were predominantly a mixture of B–V, vermiculite and kaolinite (analysis No. 23, 24, 25 in Table 2). In kaolin (plagioclase 11%) where plagioclase remains as isolated skeletal grains, fanning was completed to form long vermicular kaolinite pseudomorphs after biotite, with disappearance of lenticular voids (Figure 2E and 2F). They had high Fe_2O_3 and MgO contents (Table 2) and were loosely clustered in the places that were originally occupied by tightly interlocked fresh biotite (Figure 2E). The XRD pattern showed that the weathered biotite grains consisted mostly of kaolinite (Figure 4). Figure 2F also shows random aggregates of relatively small vermicular kaolinites directly formed from the solution without regard to biotite. These small vermicular kaolinites were characterized by a nearly ideal chemical composition (Jeong and Kim 1992). Aspect ratios of vermicular kaolinite pseudomorphs and fresh biotite were obtained by dividing the

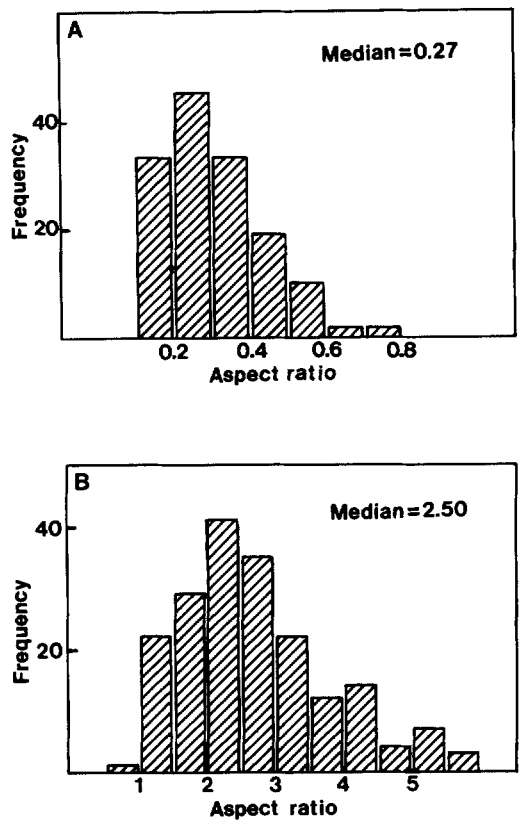

Figure 5. Diagrams showing the frequency distribution of aspect ratio of fresh biotite A) and vermicular kaolinite pseudomorph after biotite B).

grain length measured along the *c*-axis by the grain width along the basal plane in SEM photographs. The frequency distribution of aspect ratios is given in Figure 5. The median for fresh biotite was 0.27 and for vermicular kaolinites, 2.50. Since the grain widths were not changed during kaolinization, grain volume increased about 9 times after completion of kaolinization.

Sericite Kaolinization

Sericites were very finely dispersed in the anorthosite, so that they were very difficult to find under the optical microscope. But SEM photographs showed that thin flakes of sericite about 1–2 μm thick filled the microfractures (Figure 6A). Their basal planes were parallel to fracture surfaces. The fresh flakes were too thin to be analyzed by EPMA, but EDS analysis supported that they were dioctahedral mica consisting mostly of Al, Si and K. In slightly weathered friable rock (plagioclase 95%), most of the flakes were highly expanded into vermicular grains (about 20 μm) attached to each other in parallel (Figure 6B). Although the original fresh flakes were nearly invisible, the long

https://doi.org/10.1346/CCMN.1998.0460504 Published online by Cambridge University Press

Table 2. Selected EPMA data of fresh and weathered biotite.

	Fresh rock	Friable rock							
Sample no.	11	21	22	23	24	25	26	27	28
SiO_2	37.17	37.79	40.24	36.65	42.63	40.68	45.74	43.04	44.72
Al_2O_3	15.90	20.14	23.06	22.39	26.19	23.44	33.05	30.73	34.42
Fe_2O_3	18.48	12.47	12.62	15.40	10.50	11.30	3.61	5.35	3.35
MgO	13.46	5.71	4.49	5.08	4.35	5.37	0.72	2.14	1.50
TiO_2	0.73	1.71	1.25	1.56	1.21	0.81	0.03	1.18	0.22
MnO	0.02	0.06	0.11	0.07	0.53	0.06	0.00	0.00	0.00
K_2O	8.68	2.16	1.30	1.05	1.72	0.92	0.94	0.26	0.31
Na_2O	0.17	0.14	0.17	0.13	0.52	0.37	0.20	0.23	0.15
CaO	0.09	0.85	0.93	0.95	0.46	0.81	0.32	0.20	0.13
Total	94.70	81.03	84.17	83.28	88.11	83.76	84.61	83.13	84.80

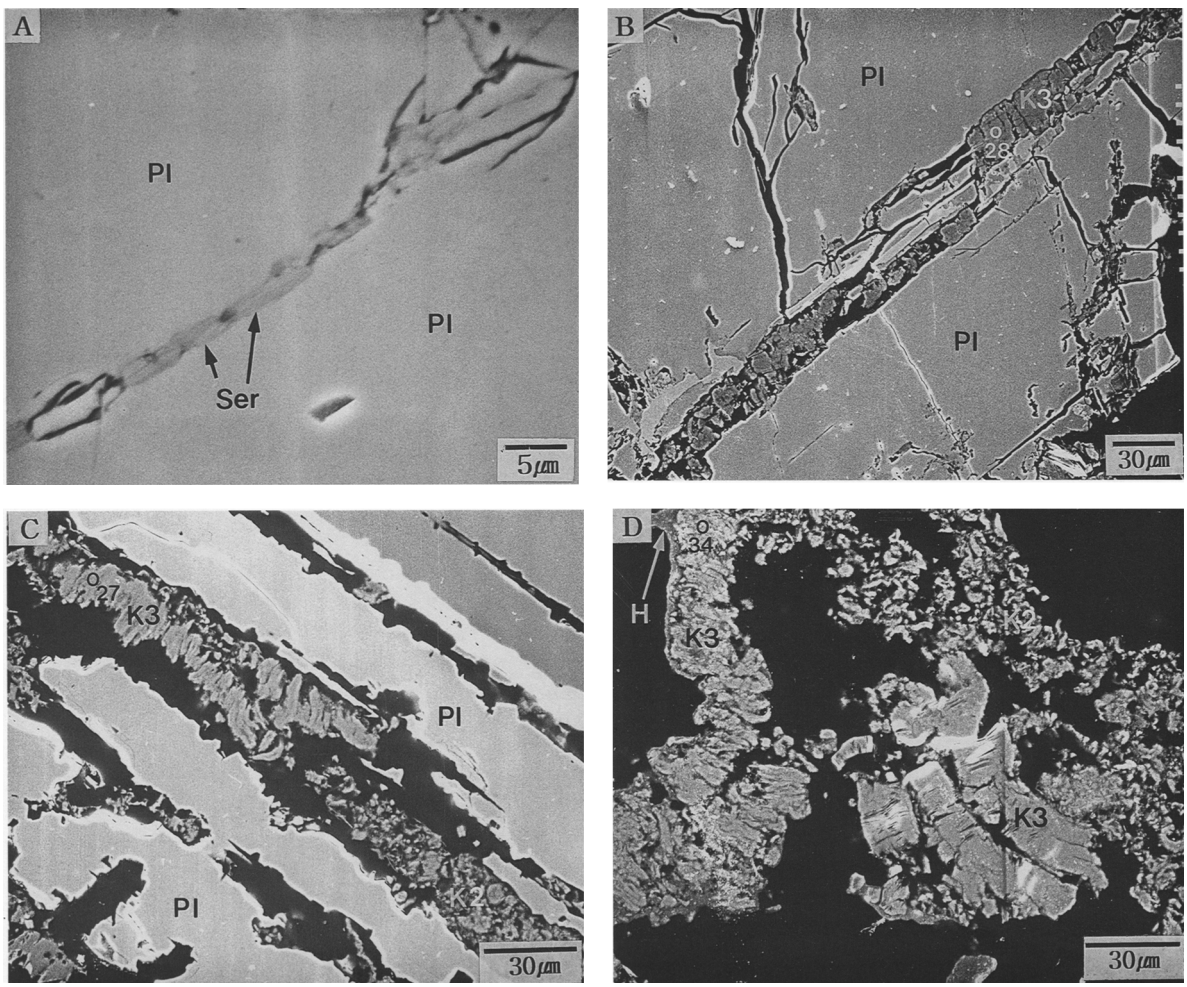

Figure 6. Scanning electron micrographs showing the kaolinizing sericite. A) Thin flakes of sericite (Ser) filling the microfractures of plagioclase (Pl) in fresh anorthosite. B) The long vermicular grains of kaolinizing sericites (K3) in the slightly weathered friable rock (plagioclase 95%). C) The vermicular grains of kaolinizing sericites (K3) separated from dissolving plagioclase (Pl) in moderately weathered friable rock (plagioclase 46%). D) The vermicular grains of kaolinizing sericites (K3) in kaolin (plagioclase 11%) forming a part of the clay wall with halloysite aggregate (H). Black = voids. Numbers beside open circle in B), C) and D) indicate the points analyzed by EPMA in Table 3.

https://doi.org/10.1346/CCMN.1998.0460504 Published online by Cambridge University Press

Table 2. Extended.

Kaolin								
31	32	33	34	35	36	37	38	39
44.65	43.74	44.46	44.13	43.54	44.73	45.75	42.72	44.98
34.80	34.84	34.58	38.28	38.78	35.78	37.58	35.84	39.24
3.42	3.24	4.15	1.34	0.52	2.62	2.06	5.90	1.40
0.84	0.95	0.99	0.28	0.25	0.95	0.36	0.61	0.16
0.17	0.18	0.01	0.03	0.05	0.05	0.02	0.12	0.02
0.04	0.06	0.08	0.03	0.03	0.00	0.04	0.00	0.00
0.10	0.13	0.05	0.07	0.10	0.09	0.10	0.04	0.07
0.11	0.10	0.10	0.09	0.09	0.08	0.08	0.04	0.12
0.11	0.10	0.11	0.03	0.05	0.19	0.10	0.10	0.02
84.24	83.24	84.53	84.28	83.41	84.49	86.09	85.37	86.01

vermicular grains were easily observed under the optical microscope. In moderately weathered friable rock (plagioclase 46%), the vermicular grains were separated from dissolving plagioclase (Figure 6C), and in highly weathered kaolin (plagioclase 11%), they became a part of the clay wall (Figure 6D). EPMA analysis confirmed that the vermicular grains were a mixture of dioctahedral mica and kaolinite (Table 3). XRD analysis of the <0.5 μm size fraction of kaolin showed, a 1*Md* dioctahedral mica–smectite mixed layer mineral with a discrete mica. Computer simulation for the mixed-layer mineral using the NEWMOD© program (Reynolds 1985) showed that 84% mica layers were interstratified with 16% smectite layers in a long-range R3 ordering pattern (Figure 7). The structural formula of the sericite concentrate analyzed by inductively coupled plasma spectrometry is $(K_{1.38}Na_{0.12}Ca_{0.08})_{1.58}(Al_{3.62}Fe^{III}_{0.10}Mg_{0.26}Ti_{0.02})_4(Si_{6.58}Al_{1.42})_8O_{20}(OH)_4$.

Clinochlore Kaolinization

The green color of clinochlore in fresh anorthosite changed to yellowish green in partially weathered anorthosite (plagioclase 46%). Clinochlore grains were partially kaolinized along layers with slight exfoliation (Figure 8A). Notable kaolinization and exfoliation were observed in the highly weathered kaolin (plagioclase 11%) (Figure 8B). Clinochlore grains were greatly exfoliated into several flakes, producing a large volume of internal voids. Each flake was subsequently cleaved into thin flakes in an anastomosis pattern, which were gradually fanned out at the edges. The edges consisted mostly of Al and Si, implying kaolin (No. 28, 29, 30 in Table 4), while the interiors contained Al, Si, Fe and Mg, implying clinochlore (No. 21, 22, 23, 24 in Table 4). The weathered grains in partially weathered anorthosite (plagioclase 46%) consisted of clinochlore, chlorite–vermiculite mixed-layer mineral (C–V) and kaolinite (Figure 9). In addition, a formamide intercalation experiment (Churchman et al. 1984) indicated the presence of halloysite as a weathering product.

Muscovite Kaolinization

Muscovite was rather resistant to weathering, so slowly weathered that it was altered only in the highly weathered kaolin (plagioclase 11%) (Figure 10). The manner of fanning was very similar to that of biotite. Kaolinization started from the edges and advanced toward the interior. Large lenticular voids were formed

Table 3. Selected EPMA data of weathered sericite

Sample no.	Friable rock								Kaolin						
	21	22	23	24	25	26	27	28	29	31	32	33	34	35	36
SiO_2	47.61	49.74	46.53	46.37	45.48	45.00	45.77	45.99	46.55	43.49	46.64	45.44	46.62	44.72	43.16
Al_2O_3	37.21	37.67	35.72	38.47	35.94	36.87	37.53	37.94	38.33	37.86	37.18	37.73	38.31	38.84	36.46
Fe_2O_3	0.54	0.49	0.57	0.50	1.11	0.53	0.42	0.52	0.60	1.07	0.60	0.44	0.14	0.03	0.19
MgO	0.52	0.21	0.31	0.09	0.20	0.07	0.09	0.08	0.23	0.29	0.28	0.04	0.09	0.03	0.04
TiO_2	0.00	0.00	0.00	0.00	0.00	0.00	0.02	0.02	0.00	0.04	0.00	0.00	0.00	0.02	0.00
MnO	0.00	0.00	0.06	0.00	0.00	0.00	0.00	0.00	0.00	0.03	0.00	0.00	0.00	0.00	0.86
K_2O	7.84	5.81	5.10	3.95	3.53	2.62	1.04	1.60	1.37	1.27	1.28	0.74	0.80	0.49	0.43
Na_2O	0.10	0.19	0.42	1.33	0.10	0.14	0.10	0.14	0.06	0.07	0.09	0.15	0.10	0.10	0.07
CaO	0.16	0.46	0.23	0.18	0.20	0.17	0.11	0.15	0.17	0.06	0.10	0.21	0.08	0.08	0.04
Total	93.96	94.57	88.94	90.89	86.55	85.40	85.08	86.44	87.31	84.18	86.17	84.75	86.14	83.81	81.25

https://doi.org/10.1346/CCMN.1998.0460504 Published online by Cambridge University Press

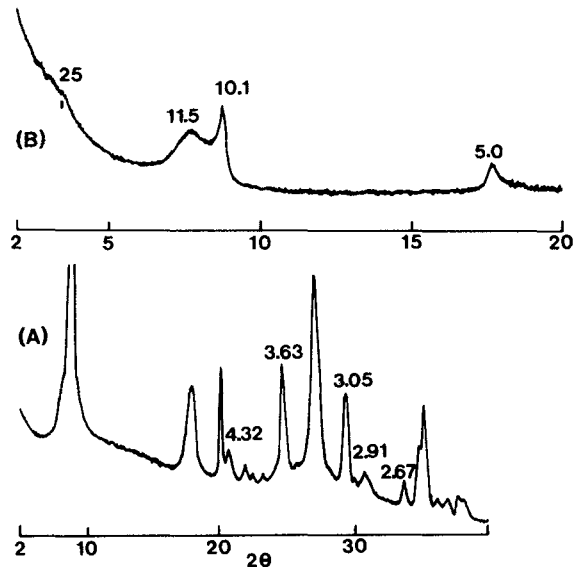

Figure 7. XRD patterns of sericite concentrate in kaolin. A) Random mount. The *d*-values over the peaks indicate diagnostic diffraction lines of 1*Md* dioctahedral mica. B) Oriented mount treated with ethylene glycol at 60 °C for 48 h.

between the exfoliated flakes, and the degree of volume increase was similar to that of biotite. The fanned edges were kaolin (analysis No. 28, 29 in Table 5), whereas the unfanned interiors were muscovite (analysis No. 21, 22 in Table 5). XRD analysis of hand-picked weathered grains, using a Debye Scherrer camera, detected muscovite and kaolinite with a small amount of vermiculite or smectite.

DISCUSSION

Diverse parent minerals were found to have altered into long vermicular kaolinite pseudomorphs simultaneously with a large increase in volume. B–V, C–V, vermiculite and smectite were formed as intermediate phases during kaolinization, but subsequently altered into kaolinite. Biotite and sericite were highly vulnerable to weathering, whereas clinochlore and muscovite were rather resistant. The mechanism and implications of kaolinization of primary phyllosilicates are discussed below.

Formation Mechanism of Vermicular Kaolinite Pseudomorphs

EPITACTIC REPLACEMENT. The destruction and reorganization of structure through a solution phase have been suggested by previous TEM studies for the kaolinization of biotite (Ahn and Peacor 1987; Banfield and Eggleton 1988) and of muscovite (Banfield and Eggleton 1990; Jiang and Peacor 1991; Singh and Gilkes 1991). Thus, dissolved elements from ambient weathering solutions can freely participate in the formation of kaolinite. Topotactic replacement only cannot give a large volume increase, so the dominance of epitactic replacement is implied to explain the intense fanning-out and resulting volume increase during alteration. Cell dimensions in the *a-b* plane of primary phyllosilicates match those of kaolinite to within 4% (Bailey 1980), so that the surface of weathering primary phyllosilicates, exposed in the finely cleaved spaces, might serve as a good template for the growth of kaolinite. The substrates of phyllosilicates facilitate the nucleation and growth of kaolinite by lowering activation energy, and epitactic overgrowth of kaolinite on the phyllosilicates has often been reported in the literature. Banfield and Eggleton (1988, 1990) suggested that kaolinite had crystallized epitactically onto biotite. Pevear and Nagy (1993) observed that kaolinite nucleates on the basal surfaces of muscovite and

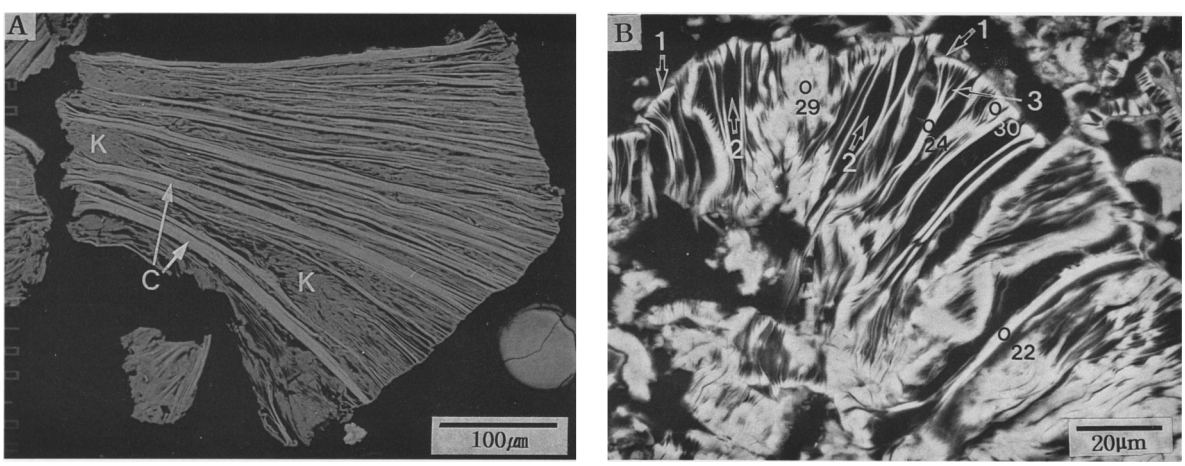

Figure 8. Scanning electron micrographs showing the kaolinizing clinochlore. A) Kaolinizing clinochlore in partially weathered anorthosite. Key: K = kaolin; C = clinochlore. B) Greatly exfoliated grains of clinochlore. Note the great fanning-out (arrows 1) and exfoliation of clinochlore with abundant large (arrows 2) and small (arrow 3) lenticular voids. Black = voids. Numbers with open circle in B) indicate the points analyzed by EPMA in Table 4.

Table 4. Selected EPMA data of weathered clinochlore in kaolin.

Sample no.	Fresh rock	Kaolin									
	11	21	22	23	24	25	26	27	28	29	30
SiO_2	26.31	23.45	25.45	26.58	28.48	39.30	42.87	41.70	43.66	44.08	43.84
Al_2O_3	20.86	22.45	20.93	20.34	22.32	30.55	35.74	33.90	33.78	36.44	34.90
Fe_2O_3	24.50	22.93	21.33	20.41	18.06	6.93	7.58	5.60	3.42	1.62	2.59
MgO	16.52	14.27	15.96	15.18	13.92	3.79	1.03	2.17	0.77	0.34	0.18
TiO_2	0.01	0.08	0.11	0.08	0.09	0.02	0.03	0.00	0.18	0.27	0.06
MnO	0.22	0.23	0.29	0.18	0.25	0.00	0.00	0.00	0.01	0.00	0.00
K_2O	0.02	0.00	0.00	0.00	0.06	0.05	0.04	0.00	0.61	0.58	0.86
Na_2O	0.01	0.00	0.00	0.02	0.03	0.11	0.09	0.06	0.23	0.16	0.15
CaO	0.00	0.02	0.07	0.29	0.36	0.30	0.04	0.19	0.61	0.14	0.17
Total	88.50	83.43	84.14	83.08	83.57	81.05	87.42	83.61	83.27	83.63	82.75

biotite in a diagenetic environment, and also simulated kaolinite overgrowth on muscovite in the laboratory; they concluded that muscovite and illite act as nucleation sites for kaolinite precipitation. Samotoin and Chekin (1993) observed the spiral growth of kaolinite on mica and chlorite substrates in weathered granite.

AI IMPORT. Assuming Al conservation, the grain volume of primary phyllosilicates should be reduced after kaolinization. Therefore, the large volume change during the kaolinization of primary phyllosilicates indicated the mass import of Al and Si from the external weathering solution into kaolinizing primary phyllosilicates. Soluble calcic plagioclase, abundant in anorthosite, would supply sufficient Al and Si to precipitate thick kaolinite packets between the finely cleaved flakes, and Al could also be transported as a dissolved species to growing sites within the weathering grains. Although Al is known to be the least mobile element in the general weathering environment, the transfer of Al on a microscopic scale has been suggested by textural studies of weathered rocks (Velbel 1989; Banfield et al. 1990; Nahon 1991).

FANNING-OUT. The kaolinization front propagated from the edges toward the interior of each grain, while continued precipitation of kaolinite at the edges produced the characteristic fanned-out textures. Great fanning from the edges exerted a tensional force on the interior, so it separated along the basal cleavages into many flakes, forming long lenticular voids. Continued kaolinization toward the interior eventually expanded the whole of each flake, so greatly increasing the volume of weathering primary phyllosilicates. The lenticular voids are transient structures appearing during the weathering of primary phyllosilicates into vermicular kaolinite, and eventually disappear with completion of kaolinization. The schematic diagram in Figure 11 shows the general process of formation of long vermicular kaolinite pseudomorphs from primary phyllosilicates.

Volumetric and Mineralogical Contributions

Weathering of primary phyllosilicates, even where initial content is small, contributes greatly to the formation of vermicular kaolinite in a weathering environment. This can be exemplified by the weathering of anorthosite containing 1 vol% of biotite in the studied weathering profile. Porosity of the kaolin was 52 vol%. Assuming isovolumetric weathering, the 9-fold volume increase of weathered biotite means that even

Table 5. Selected EPMA data of weathered muscovite in kaolin.

Sample no.	Fresh rock	Kaolin								
	11	21	22	23	24	25	26	27	28	29
SiO_2	45.95	44.54	43.45	41.28	44.13	47.78	42.25	46.50	44.77	45.06
Al_2O_3	31.25	31.79	31.71	28.48	34.40	35.12	35.62	35.89	34.63	36.79
Fe_2O_3	3.54	2.81	2.24	2.31	1.61	0.90	1.12	0.88	0.90	1.63
MgO	1.43	1.21	0.94	1.34	1.29	0.53	0.07	0.43	0.15	0.10
TiO_2	0.04	0.28	0.23	0.41	0.30	0.02	0.02	0.03	0.00	0.03
MnO	0.00	0.00	0.05	0.00	0.37	0.00	0.00	0.00	0.00	0.00
K_2O	9.77	10.93	7.20	4.26	4.61	4.33	3.50	3.09	0.57	0.13
Na_2O	0.19	0.33	0.23	0.65	0.17	0.24	0.48	0.18	0.15	0.07
CaO	0.00	0.00	0.07	0.12	0.16	0.19	0.10	0.11	0.09	0.16
Total	92.25	91.95	86.07	78.85	87.04	89.11	83.16	87.11	81.26	83.97

https://doi.org/10.1346/CCMN.1998.0460504 Published online by Cambridge University Press

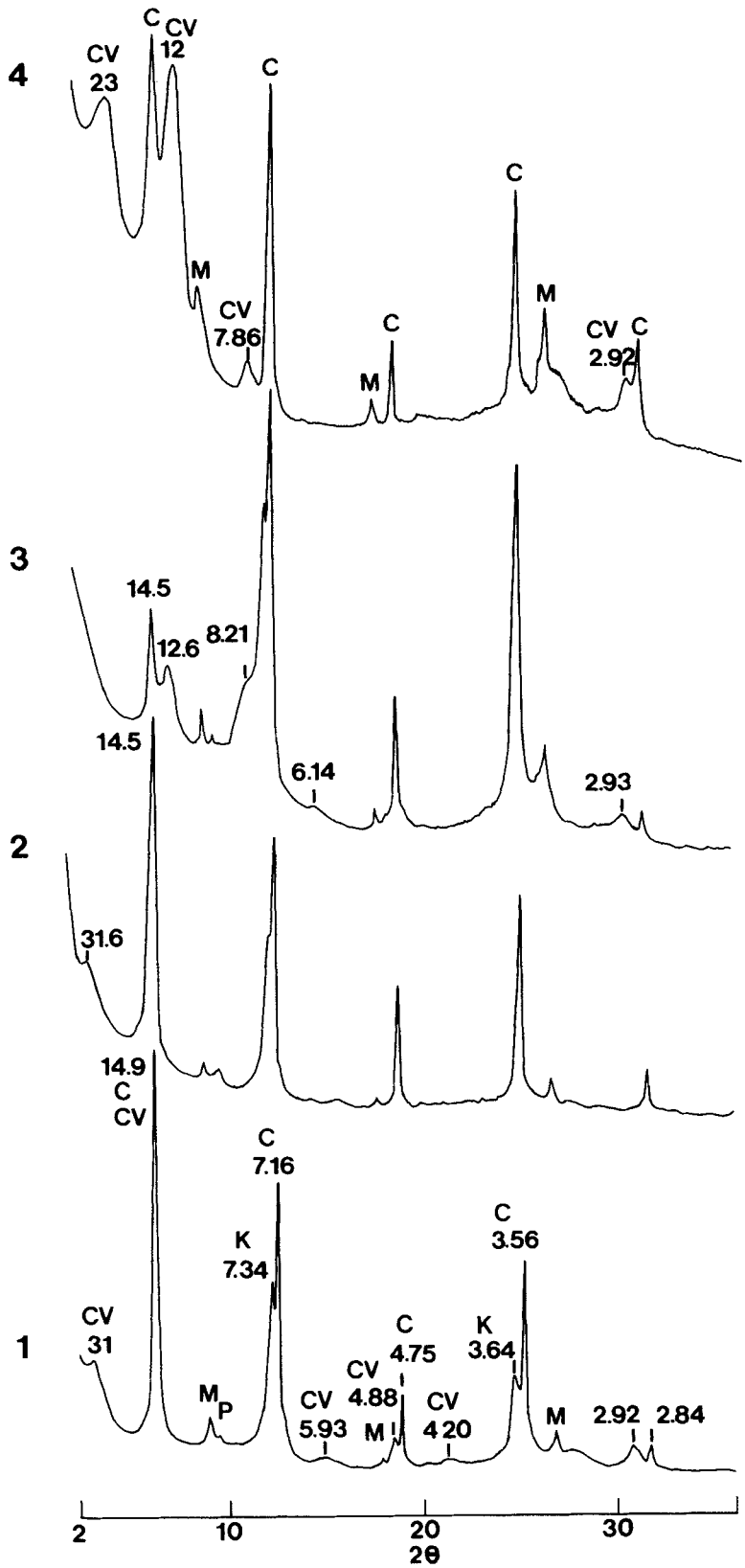

https://doi.org/10.1346/CCMN.1998.0460504 Published online by Cambridge University Press

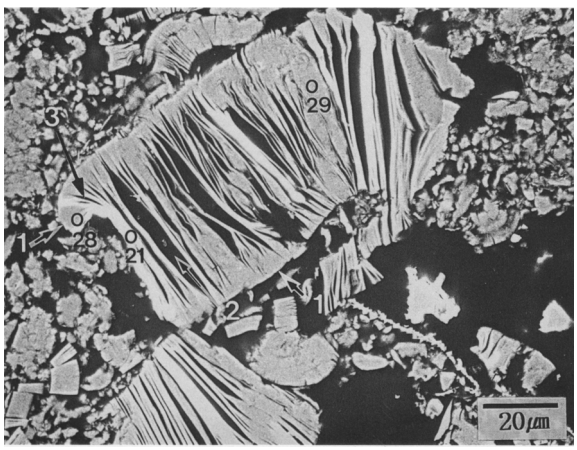

Figure 10. Scanning electron micrograph showing the kaolinizing muscovite in kaolin. Note the great fanning-out (arrows 1) and exfoliation of muscovite grains with abundant large (arrow 2) and small (arrow 3) lenticular voids. Black = voids. Numbers beside open circle indicate the points analyzed by EPMA in Table 5.

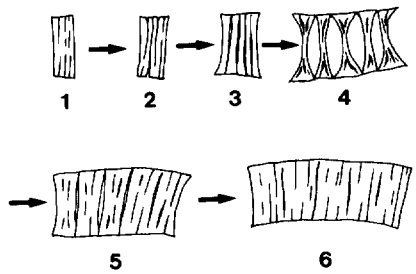

Figure 11. A schematic diagram showing the general process of formation of long vermicular kaolinite pseudomorphs. 1. Fresh grain, 2. Partial transformation into expandable clays without notable volume changes, 3. Beginning of kaolinization from edges, 4. Great fanning-out from the edges resulting in lenticular voids, 5. Disappearance of the lenticular voids with propagation of fanning-out toward the interior of flakes, 6. Final formation of long vermicular kaolinites.

1 vol% of biotite in anorthosite contributes 17 vol% of the solid part of weathered anorthosite as a vermicular kaolinite. Since the total kaolinite content of the kaolin was 53 wt% (Table 1), about 31 wt% of kaolinite content was estimated to be formed by biotite weathering. While true volume may be reduced slightly by the invisible micropores in vermicular kaolinite, a 9-fold increase in volume is highly significant. The major role of primary phyllosilicates in the weathering process was to allow the thick epitactic overgrowth of kaolinite to form expanded vermicular grains. It is notable that the volume change of whole rock was very small despite the large volume increase of the weathering primary phyllosilicates. The increased volume must be compensated by voids produced by the dissolution of plagioclase which is the major mineral of the anorthosite. The significant volumetric and mineralogical contributions of primary phyllosilicates to the kaolinization are supported by the statistical analysis of the chemistry of clays by Weaver and Pollard (1973) in which vermicular kaolinite books in Georgia hard kaolin are positively correlated with mica content. Vermicular grains are the common habit of kaolinite in weathering and diagenetic environments, but their diverse origins have not been clarified in previous studies (Keller 1977; Murray 1988). Many of the vermicular kaolinites described from low-temperature geological environments are probably the expanded pseudomorphs after primary phyllosilicates that have undergone fanning and exfoliation. High activity of Al in the ambient solution promotes thick epitactic overgrowth of kaolinite on the templates of primary phyllosilicates. Minor residual elements inherited from parent minerals may indicate the origin of vermicular kaolinites: K from sericite and muscovite, Fe and Mg from chlorite and biotite. These elements exist as inclusions of parent minerals between kaolinite layers (Lee et al. 1975) or in the kaolinite structure (Jepson and Rouse 1975).

CONCLUSION

Primary phyllosilicates were altered into kaolinite through the short stage of intermediate phases. Kaolinization began at grain edges and propagated toward interiors. The large volume increase during kaolinization indicated that a large amount of Al was transferred from dissolving plagioclase into weathering primary phyllosilicates. Thick epitactic growth of kaolinite on the templates of primary phyllosilicates forced the original grains to expand greatly, forming long vermiform kaolinite pseudomorphs via exfoliation and fanning-out. The primary phyllosilicate content of anorthosite was very low, so their elemental contributions to the kaolinic weathering profiles could only be small. But as a template facilitating the precipitation of kaolinite, they made significant volumetric and mineralogical contributions.

ACKNOWLEDGEMENTS

The author thanks W. D. Nettleton, D. R. Pevear and an Associate Editor for their critical reviews. S. J. Kim is thanked for introducing the author to clay mineralogy. This work was supported by the Basic Science Research Institute

←

Figure 9. XRD patterns of kaolinizing clinochlore. Oriented mounts. 1: raw sample; 2: Mg-saturation and ethylene glycol treatment at 60 °C for 48 h; 3: heating at 370 °C for 4 h; 4: heating at 370 °C for 4 h. Key: C = chlorite; CV = chlorite–vermiculite mixed layer mineral; K = kaolinite; M = muscovite.

Program, Ministry of Education, Korea (project No. BSRI 97-5402).

REFERENCES

Ahn JH, Peacor DR. 1987. Kaolinitization of biotite: TEM data and implications for an alteration mechanism. Am Mineral 72:353–356.

Bailey SW. 1980. Structure of layer silicates. In: Brindley GW, Goodman G, editors. Crystal structures of clay minerals and their X-ray identification. London: Mineral Soc. p 1–124.

Banfield JF, Eggleton RA. 1988. Transmission electron microscope study of biotite weathering. Clays Clay Miner 36: 47–60.

Banfield JF, Eggleton RA. 1990. Analytical transmission electron microscope studies of plagioclase, muscovite, and K-feldspar weathering. Clays Clay Miner 38:77–89.

Banfield JF, Veblen DR, Jones BF. 1990. Transmission electron microscopy of subsolidus oxidation and weathering of olivine. Contrib Mineral Petrol 106:110–123.

Brindley GW. 1980. Order-disorder in clay mineral structures. In: Brindley GW, Brown G, editors. Crystal structures of clay minerals and their X-ray identification. London: Mineral Soc. p 125–195.

Cho HD, Mermut AR. 1992. Evidence of halloysite formation from weathering of ferruginous chlorite. Clays Clay Miner 40:608–619.

Churchman GJ, Whitton JS, Claridge GGC, Theng BKG. 1984. Intercalation method using formamide for differentiating halloysite from kaolinite. Clays Clay Miner 32:241–248.

Coffman CB, Fanning DS. 1975. Maryland soils developed in residuum from chlorite metabasalt having high amounts of vermiculite in sand and silt fractions. Soil Sci Soc Am J 39:723–732.

Eswaran H, Bin WC. 1978. A study of a deep weathering profile on granite in Peninsular Malaysia: III. Alteration of feldspars. Soil Sci Soc Am J 42:154–158.

Fordham AW. 1990. Formation of trioctahedral illite from biotite in a soil profile over granite gneiss. Clays Clay Miner 38:187–195.

Gilkes RJ, Suddhiprakarn A. 1979a. Biotite in deeply weathered granite. I. Morphologic, mineralogical, and chemical properties. Clays Clay Miner 27:349–360.

Gilkes RJ, Suddhiprakarn A. 1979b. Biotite in deeply weathered granite. II. The oriented growth of secondary minerals. Clays Clay Miner 27:361–367.

Harris WG, Zelazny JC, Baker JC, Martens DC. 1985. Biotite kaolinitization in Virginia Piedmont soils: I. Extent, profile trends, and grain morphological effects. Soil Sci Soc Am J 49:1290–1297.

Harris WG, Zelazny JC, Bloss FD. 1985. Biotite kaolinitization in Virginia Piedmont soils: II. Zonation in single grains. Soil Sci Soc Am J 49:1297–1302.

Jeong GY. 1992. Mineralogy and genesis of kaolin in the Sancheong district, Korea [Ph.D. thesis]. Seoul, Korea: Seoul National Univ. 325 p.

Jeong GY, Kim SJ. 1992. Kaolinites in the Sancheong kaolin, Korea: Their textures, chemistry, and origin. In: Nagasawa K, editor. Clay minerals, their natural resources and uses. Proc Workshop WB-1; 29th Int Geol Cong; 1992; Nagoya, Japan. p 129–135.

Jeong GY, Kim SJ. 1993. Boxwork fabric of halloysite-rich kaolin formed by weathering of anorthosite in Sancheong area, Korea. Clays Clay Miner 41:56–65.

Jepson WB, Rouse JB. 1975. The composition of kaolinite—An electron microscope microprobe study. Clays Clay Miner 23:310–317.

Jiang WT, Peacor DR. 1991. Transmission electron microscopic study of the kaolinitization of muscovite. Clays Clay Miner 39:1–13.

Keller WD. 1977. Scan electron micrographs of kaolins collected from diverse environments of origin. IV. Georgia kaolin and kaolinizing source rocks. Clays Clay Miner 25: 311–345.

Konta J. 1972. Secondary illite and primary muscovite in kaolins from Karlovy Vary area, Czechoslovakia. In: Serratosa JM, editor. Proc Int Clay Conf; 1972; Madrid, Spain. Madrid: Div Ciencias, CSIC. p 143–157.

Korea Meteorological Service. 1985. Climatic summary of Korea. Seoul, Korea: Korea Meteorological Service. p 220.

Kwon ST, Jeong JG. 1990. Preliminary Sr-Nd isotope study of the Hadong-Sanchung anorthositic rocks in Korea: Implication for their origin and for the Precambrian tectonics. J Geol Soc Korea 26:341–349.

Lee SY, Jackson ML, Brown JL. 1975. Micaceous inclusions in kaolinite observed by ultramicrotomy and high resolution electron microscopy. Clays Clay Miner 23:125–129.

Murray HH. 1988. Kaolin minerals: Their genesis and occurrences. In: Bailey SW, editor. Hydrous phyllosilicates. Rev Mineral 19. Washington: Mineral Soc Am. p 67–89.

Nahon DB. 1991. Introduction to the petrology of soils and chemical weathering. New York: J. Wiley. 313 p.

Pevear DR, Nagy KL. 1993. Kaolinite growth on mica in sandstones, bentonites, and experiments. In: Abstr 10th Int Clay Conf; 1993; Adelaide, South Australia. O-141.

Rebertus RA, Weed SB, Buol SW. 1986. Transformation of biotite to kaolinite during saprolite—Soil weathering. Soil Sci Soc Am J 50:810–819.

Reynolds RC, Jr. 1985. NEWMOD©—A computer program for the calculation of one-dimensional diffraction patterns of mixed-layered clays. 8 Brook Dr., Hanover, New Hampshire: R. C. Reynolds, Jr.

Robertson IDM, Eggleton RA. 1991. Weathering of granitic muscovite to kaolinite and halloysite and of plagioclase-derived kaolinite to halloysite. Clays Clay Miner 39:113–126.

Samotoin ND, Chekin SS. 1993. Helical growth of kaolinite crystal in layer silicates. In Abstr 10th Int Clay Conf; 1993; Adelaide, South Australia. P-143.

Singh B, Gilkes RJ. 1991. Weathering of a chromian muscovite to kaolinite. Clays Clay Miner 39:571–579.

Stoch L, Sikora W. 1976. Transformations of micas in the process of kaolinitization of granites and gneisses. Clays Clay Miner 24:156–162.

Velbel MA. 1989. Weathering of hornblende to ferruginous products by a dissolution-precipitation mechanism: Petrography and stoichiometry. Clays Clay Miner 37:515–524.

Weaver CE, Pollard LD. 1973. The chemistry of clay minerals. Amsterdam, Netherlands: Elsevier. 213 p.

(Received 23 December 1996; accepted 23 January 1998; Ms. 2843)